Advances in Nano Research, *Vol. 11, No. 1 (2021) 73-81*
https://doi.org/10.12989/anr.2021.11.1.073

Synthesis of hairpin DNA mediated Au-Ag bimetallic nanomushrooms for antibacterial application

Jingtai Fu[#], Lu Huang[#], Zhongning Yu, Zhuomin Zhang[*] and Gongke Li[**]

School of Chemistry, Sun Yat Sen University, Guangzhou 510275, China

(*Received January 4, 2020, Revised April 6, 2021, Accepted May 11, 2021*)

Abstract. Precise control of the synthesis of bimetallic nanoparticles with specific morphology and structure is of great significance due to their excellent catalytic, optical and biological property. DNA molecules are considered as a kind of efficient templates to mediate the precise synthesis of bimetallic nanoparticles with homogeneous morphology due to their specific and controllable structure. In this study specific hairpin DNA strands were successfully utilized as templates to mediate the synthesis of special mushroom-like Au-Ag bimetallic nanoparticles with a high yield of > 90%. Several key factors greatly influencing the precise control of the morphology and UV-Vis characteristics of the proposed Au-Ag nanomushrooms during synthesis were investigated and optimized in detail, including the structure of template DNA, loading amounts of DNA, types of reductant agents and surfactants. Then, the formation mechanism of hairpin DNA mediated Au-Ag nanomushrooms was studied. Finally, the proposed Au-Ag nanomushrooms with good biocompatibility were applied for the antibacterial study by the growth curve of E. coli. The proposed Au-Ag nanomushrooms showed the effective inhibition capability for the growth of E. coli. The results suggested that these DNA mediated Au-Ag nanomushrooms possessed great potential applications for biomedical science in future.

Keywords: antibacterial study; Au-Ag bimetallic nanomushrooms; biocompatibility; hairpin DNA mediated

1. Introduction

Bimetallic nanoparticles have been widely applied in the range of catalysis (Ma *et al*. 2016) (Kim *et al*. 2017), chemical sensing (Mandal *et al*. 2018) (Gilroy *et al*. 2016) and bioimaging (Zhang *et al*. 2017, 2018) due to their unique physical and chemical properties, and these properties are closely related to their bimetallic composition, morphology and structure. Compared with single metal nanoparticles, bimetallic nanoparticles not only possess higher physical and chemical stability, but also showed the emerging priorities due to the synergistic effect between the two metals (Zaleska *et al*. 2016). In recent years, the synthesis and application of bimetallic nanoparticles with different compositions and morphologies have been a hot line in nanoscience, including Au-Ag (Yin *et al*. 2018), Au-Cu (Niu *et al*. 2017), Ag-Cu (Li *et al*. 2018), Au-Pt (Jawad *et al*. 2019), Pd-Au (Lu *et al*. 2018), etc. Among them, Au-Ag bimetallic nanoparticles attracted the researchers most, since Au and Ag nanoparticles have a similar catalytic structure with face-centered cubic lattice, making Au-Ag bimetallic nanoparticles have higher catalytic activity (Berahim *et al*. 2018). Besides, the localized surface plasmon resonances (LSPR) bands of Au-Ag bimetallic nanoparticles are generally located in the visible region due to the conversion of d-d band, which makes them particularly suitable for biological applications (Liz *et al*. 2006).

At present, several synthesis strategies of bimetallic nanoparticles have been reported, including coreduction (Chi *et al*. 2015), seed-mediated growth (Xia *et al*. 2017), galvanic replacement reaction (Da Silva *et al*. 2017) and template method (Taylor *et al*. 2017). And many different morphologies of bimetallic nanoparticles have been obtained. For example, Au@Ag heterogeneous nanorods (NRs) were synthesized by the co-reduction of $HAuCl_4$ and $AgNO_3$ in ethylene glycol solution, and the bimetallic Au@Ag heterogeneous NRs were applied for one-pot analysis of glucose at nearly neutral pH (Han *et al*. 2015). Zhao *et al*. (2017) synthesized a kind of multi-branch Au-Ag bimetallic core-shell-satellite nanoparticles, and the structure was used as SERS substrate for thiram detection. Although there have been many reports on the synthesis of bimetallic nanoparticles, many synthetic parameters are often interdependent and difficult to be tuned accurately. Thus, it is still a great challenge to precisely control the morphologies and plasmonic properties of bimetallic nanoparticles at nanoscale. Template method usually utilizes the mild reaction conditions for synthesis of specific nanostrutures, and the synthesis process is relatively easy to be controlled (Wang *et al*. 2017). Besides, this method has the advantages of low cost, fast reaction rate and easy large-scale synthesis (Fan *et al*. 2017). Therefore, template method would be the suitable

*Corresponding author, Ph.D.,
E-mail: zzm@mail.sysu.edu.cn
**Co-corresponding author, Ph.D.,
E-mail: cesgkl@mail.sysu.edu.cn
[#]These authors contributed equally to this work.

ISSN: 2287-237X (Print), 2287-2388 (Online)

and efficient way for the precise synthesis of bimetallic nanoparticles.

As a kind of biomacromolecules, DNA has regular and controllable structures. In addition to single and double strands, DNA can form other structures including hairpins, G-quadruplexes and i-motifs (Yatsunyk *et al*. 2014). These structures not only increase the diversity of DNA microstructure, but also improve the thermal and chemical stability of DNA molecules. Thus, DNA has advantages as a template for the synthesis of bimetallic nanoparticles with specific morphology. Several studies on DNA mediated noble metal nanoparticles have been reported in recent years (Wang *et al*. 2010, Song *et al*. 2015, Fu *et al*. 2019). Lu research group used four different 10-base homooligomer DNA strands containing A, G, C, and T as templates to mediate palladium nanocube growth, and four different morphologies of Pd-Au bimetallic nanoparticles were obtained (Satyavolu *et al*. 2016). They found that template DNA controlled the morphologies by affecting the binding affinity with Pd nanocubes and the diffusion of $HAuCl_4$ from the solution to the surface of Pd nanocubes. Nam and coworkers (Lim *et al*. 2008) synthesized DNA-embedded Au-Ag core-shell bimetallic nanoparticles, and the shell thicknesses and plasmonic properties of Au-Ag core-shell bimetallic nanoparticles could be tuned by changing the DNA sequence and the amount of $AgNO_3$. They also found that the morphology of DNA mediated Au-Ag bimetallic nanoparticles was also affected by the concentration of NaCl (Lee *et al*. 2012, 2014). Due to its weak rigidity, single-stranded DNA was easily coated on the surfaces of nanoseeds, which made it difficult to form multi-branched structures (Tan *et al*. 2015). Double-stranded DNA was more rigid than single-stranded DNA, so it tended to be more easily erected on the surface of nanoseeds for precisely regulating the growth of metal nanoparticles with high surface roughness. Ma *et al*. (Ma *et al*. 2016) synthesized double-stranded DNA mediated gold nanocrystals with defined topologies such as pushpin-, star- and biconcave disk-like structures via anchoring double-stranded DNA onto gold nanoseeds. Zhang *et al*. (2019) used three different structures of DNA as templates to precisely control the growth of gold nanorods and finally obtained trepang-like gold nanocrystals, which were applied for imaging analysis.

The morphology and geometric configuration of bimetallic nanoparticles can be precisely tuned by controlling the structure and composition of template DNA, which will affect their plasmonic properties and biomedical properties (Chen *et al*. 2018). In this study, we designed a series of hairpin DNA strands anchored onto gold nanoseeds to regulate the deposition of sliver nanoparticles. The homogeneous morphology of Au-Ag bimetallic nanoparticles was finely tuned to a special nanomushroom by precisely regulating the template DNA. The relationship between the morphology of Au-Ag bimetallic nano-mushrooms and DNA composition was comprehensively analyzed by TEM and UV-Vis. It was found that the structure of template DNA, loading amounts of DNA, types of reductant agents and surfactants had significant effects on the morphology of Au-Ag bimetallic nanomushrooms. And the growth mechanism of Au-Ag bimetallic nanomushrooms was also discussed in the paper. Finally, Au-Ag bimetallic nanomushrooms with good bio-compatibility were applied to inhibit the growth of E. coli, indicating their potential priority in biomedical application.

2. Experimental

2.1 Reagents and instruments

Hydrochloric acid (HCl) (AR, 12.1 mol/L), L-ascorbic acid (L-AA) (AR, 99.0%) and sodium chloride (NaCl) (AR, 99.5%) were purchased from Guangzhou Chemical Reagent Factory (Guangzhou, China). Silver nitrate ($AgNO_3$) (AR, 99.8%) and polyvinylpyrrolidone (PVP) (Average molecular weight 58000, K29-32) were purchased from Shanghai Aladdin Biochemical Technology Co., Ltd (Shanghai, China). Tris (Molecular Biology Grade, 99.9%), Tween-20 (GR, 1.095 g/mL), Tween-80 (GR, 1.08 g/mL) and DNA (HPLC Grade) were purchased from Sangon Biotech (Shanghai) Co., Ltd. Escherichia coli (ATCC 8739) were purchased from Guangdong Culture Collection Center (Guangzhou, China). Spherical gold nanoparticles were purchased from the US Ted Pella company (Redding, USA) with the concentration of 1.16 nM. The other reagents were analytical pure. Ultrapure water (>18.25 MΩ) was used in all experiments.

UV-Vis absorption spectra of Au-Ag bimetallic nanomushrooms aqueous solutions were recorded by a Shimadzu UV-2600 spectrophotometer with QS-grade quartz cuvettes at the wavelength range of 300-700 nm. Transmission electron microscopic (TEM) images were acquired on TEM operated at an accelerating voltage of 120 kV (FEI Tecnai G2 Spirit). The Zeta potential analyzer (Brookhaven NanoBrook 90Plus PALS) was used to estimate the Zeta potentials (ζ) of hp5 DNA-Au NPs with different loading amounts.

2.2 Preparation of hairpin DNA modified AuNPs

Firstly, five series of hairpin DNA (hp DNA) sequences were annealed based on the corresponding SH decorated single-stranded DNA (shown in Table 1). In detail, 10.0 μL of 100.0 μM thiol-DNA solution was mixed with 40.0 μL of 10.0 mM Tris-HCl solution (pH = 7.42). Afterwards, the mixture was heated to 95℃ and maintained for 5 min, and then naturally cooled down to 25℃. Then, 100.0 μL of 20% Tween-20 solution was mixed with 1.0 mL of 1.16 nM AuNPs solution, and the mixture was shaken for 5 min. Then, a certain amount of 20.0 μM hp DNA solution was added to the solution and kept at room temperature for 30 min. After that, 100.0 μL of 5.0 M NaCl solution was added to the solution, and the resulting solution was incubated in dark for 48 h at room temperature. At last, the solution was centrifuged at 13000 g for 20 min followed by removing the supernatant and rinsing the precipitate with 1.0 mL of H_2O. The centrifugation and rinsing procedures were repeated for 3 times. Finally, the precipitate was dispersed with 1.5 mL of H_2O, and the prepared hp DNA-AuNPs were kept in dark at 4℃.

2.3 Synthesis and characterization of Au-Ag bimetallic nanomushrooms

Firstly, 20.0 μL of hp DNA modified AuNPs solution was mixed with 100.0 μL of 1% PVP. After that, 60.0 μL of 50.0 mM L-AA and 30.0 μL of 1 mM $AgNO_3$ were added, followed by being vigorous vortexed for 15 s. Then, the mixture was incubated in dark for 5 min to obtain the Au-Ag bimetallic nanomushrooms. Au-Ag nanomushrooms synthesized were characterized by a TEM (Tecnai G2 Spirit 120 kV, FEI, Netherlands) and UV-vis spectrophotometer (UV-2600, Shimadzu, Japan). The TEM samples were prepared by dropping the resulted solution onto the copper grid. After being dried at room temperature overnight, the images of samples were recorded by TEM. Accordingly, 50.0 μL of the resulted solution were added in a biodrop cuvette followed by scanning their UV intensities at room temperature at wavelength from 300 to 700 nm.

2.4 Quantification of hp DNA loading on AuNPs

The number of hp DNA strands conjugated to AuNP surface was quantified by fluorescence spectroscopy with Oligreen reagent (Demers *et al*. 2000). Firstly, 25.0 μL of as-prepared hp DNA modified AuNPs were mixed with 25.0 μL of 2-mercaptoethanol solution and 200.0 μL of PBS solution followed by being incubated in dark at room temperature overnight. Before the test, a series of standard solutions of different hp DNA strands were prepared in PBS with the concentrations of 1.0, 5.0, 10.0, 20.0, 40.0, 60.0 and 80.0 nM. Then, 50.0 μL of the overnight solutions of the hp DNA modified AuNPs or the standard solutions were mixed with 50.0 μL of prepared Oligreeen stock (25.0 μL of Oligreeen in 4.975 mL of TE buffer) for the fluorescence detection. After that, 5.0 μL of 2-mercaptoethanol solution and 50.0 μL of Oligreeen stock were added into 45.0 μL of PBS to prepare the blank sample. The Oligreen fluorescence of all the samples was measured by a Microplate Reader using excitation wavelength of 480 nm and emission wavelength of 520 nm. According to the standard linear calibration curve prepared by different concentrations of hp DNA standard solution, the fluorescence of hp DNA released could be converted to corresponding hp DNA concentration. Finally, the loading amounts of DNA can be calculated based on the calibration curve. The purpose of adding 2-mercaptoethanol in the Oligreen analysis technology was to use the strong bond cooperation between 2-mercaptoethanol and AuNPs to desorb DNA loaded on the surface of gold nanoparticles through competitive adsorption.

2.5 Cytotoxicity assessment

The viability of HeLa cells was measured by the cell counting kit 8 (CCK-8) test. Firstly, 100.0 μL of cell suspension was dripped in a 96-well plate and incubated at 37℃ for 24 h. Then, Au-Ag nanomushrooms with different concentrations of 0.1, 0.2, 0.3, 0.4, 0.5, 0.6, 0.7, 0.8 nM were added and incubated for another 6 h. After that, the medium was replaced with fresh culture media that contained 10.0 μL of CCK-8 solution followed by being incubated for 2 h. Finally, the O.D values of cells at 450 nm were measured by the microplate reader.

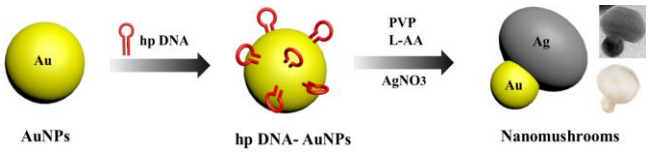

Fig. 1 Schematic of the synthesis strategy of Au-Ag bimetallic nanomushrooms

2.6 Antibacterial property of Au-Ag bimetallic nanomushrooms

E. coli cells were activated in Luria Broth at 37°C for 18 h. To examine the inhibition effect of Au-Ag nano-mushrooms on bacterial growth kinetics, 2.0 mL of bacterial suspension with proper concentration was added to the culture tube. Then, *E. coli* cells were grown in culture tube at 37°C with continuous agitation until the population of bacteria reached 10^6 CFU/mL. Finally, 200.0 μL of as-prepared Au-Ag nanomushrooms were added to the solution, and bacterial growth kinetics were determined by measuring the O.D values at 600 nm.

3. Results and discussion

3.1 Synthesis strategy of Au-Ag bimetallic nanomushrooms

Au-Ag bimetallic nanoparticles are of greater interest than monometallic nanoparticles in terms of their enhanced catalytic and optical properties, due to the synergistic effect between the two metals. It is an effective method to synthesize Au-Ag bimetallic nanoparticles with different morphologies by DNA template mediated deposition of Ag nanoparticles onto Au seeds. Compared with single-stranded DNA, hp DNA has stronger rigidity and larger structure, thus affecting the nucleation and growth of silver precursors on gold surfaces. In this study, AuNPs were used as the core to bond with five different template hp DNAs using L-ascorbic acid as the reducing agent and PVP as the surfactant. It was interesting that hp DNA strands with larger loop or longer stem as template would result in Au-Ag bimetallic nanomushrooms. The synthesis strategy of Au-Ag bimetallic nanomushrooms is shown in Fig. 1.

3.2 Optimization of synthesis conditions

Template method is an effective strategy for the synthesis of bimetallic nanoparticles (Madsen *et al*. 2019). The types of reducing agents and surfactants used in the synthesis process, as well as the structure of the template, have an important influence on the morphology and characteristics of the bimetallic nanoparticles obtained. Different reducing agents have different reducing capacities, affecting the growth rate of silver nanoparticles during synthesis and further specific morphologies. If the reduction rate is too fast, it will be difficult for silver nanoparticles to deposit in a specific direction, and core-

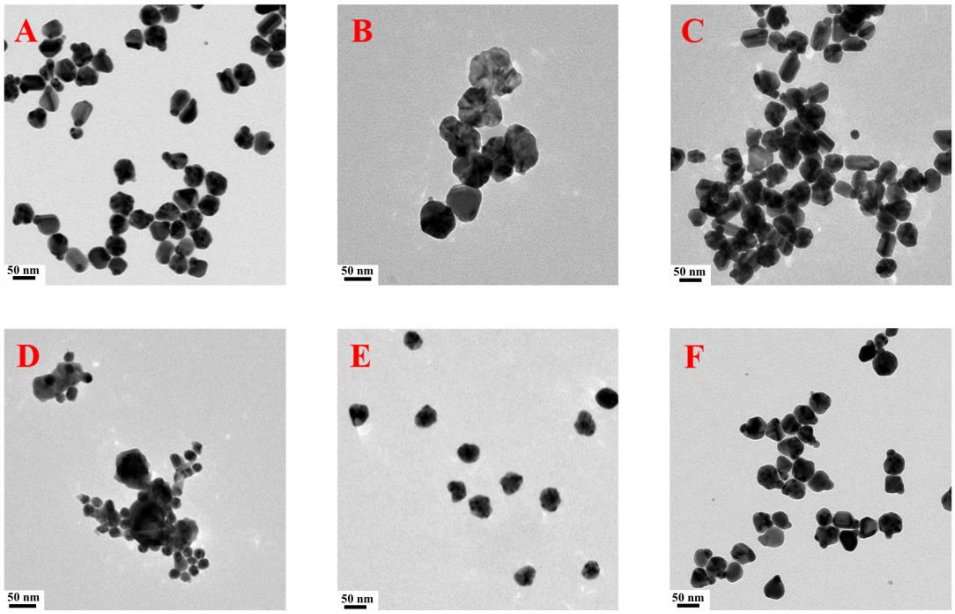

Fig. 2 TEM images of hp5 DNA mediated Au-Ag bimetallic nanoparticles using different reducing agents including L-ascorbic acid (A), sodium borohydride (B) and hydroquinone (C) and without (D) or with the addition of different surfactant including Tween-20 (E) and polyvinylpyrrolidone (F)

shell structure will be formed. Therefore, as a mild reductant L-ascorbic acid was selected to control the growth rate of silver nanoparticles during synthesis in this study. It could be seen from Fig. 2 that L-ascorbic acid as reductant would facilitate the growth of Au-Ag bimetallic nanomushrooms, while sodium borohydride or hydroquinone as reductant would result in the growth of core-shell Au-Ag nanoparticles but not nanomushrooms.

Surfactant has a great influence on the growth process and final morphology of nanoparticles (Martinsson *et al*. 2016). Surfactants with different structures and charges would generate the different affinity force between metal-surfactant complexes and nanoseeds which would greatly influence the growth process of nanoseeds and the final morphology of nanoparticles. In this study, the effects of Tween-20, PVP and non-surfactant on the synthesis of Au-Ag bimetallic nanoparticles were investigated. It could be seen obviously from Fig. 2 that without the addition of surfactant, the resulted Au-Ag nanoparticles were aggregated (Fig. 2(D)), and the addition of surfactant of Tween-20 would facilitate the growth of regular nanospheres (Fig. 2(E)). When PVP was used as surfactant during synthesis, the expected Au-Ag nanomushrooms were formed (Fig. 2(F)). Because the surfactant of PVP in the synthetic system not only acted as stabilizing agent, but also could form a large Ag-PVP complex through coordination bond, resulting in the asymmetric deposition of silver nanoparticles on the surface of gold nanoseeds and eventually forming Au-Ag nanomushrooms (Habibi *et al*. 2010) (Wang *et al*. 2005). Thus, PVP was chosen as the optimal surfactant for the synthesis of Au-Ag nanomushrooms.

The different bases composition and structure of template DNA may affect the charge distribution and spatial state on the surface of nanoseeds, thus affecting the subsequent reduction and deposition of metal precursors, and resulting in the formation of metal nanoparticles with various morphologies (Satyavolu *et al*. 2019). In this study, we designed five different hp DNA sequences (Table 1) to conjugate with Au NPs at the same feeding ratio to synthesize hp DNA-AuNPs. Then, silver ions were reduced on the surface of hp DNA-AuNPs to obtain various Au-Ag bimetallic nanoparticles. It could be seen from Fig. 3 that the morphology of hp2, hp3 and hp5 DNA mediated Au-Ag nanoparticles was nanomushroom-like, while the morphology of hp1 and hp4 DNA mediated Au-Ag nanoparticles was nanosphere-like. The UV-Vis spectra (Fig. 3(F)) showed that the resonance peaks of Au-Ag nanoparticles were strongly affected by the structure of template DNAs. And the resonance peak corresponded to both the transverse surface plasmon resonance of the AuNPs and the capacitive plasmon mode due to the coupling of the charges piled up between the junction of Au and AgNPs (Lee *et al*. 2014). It was seen that there were two resonance peaks at 420 nm and 555 nm in the UV-Vis spectra of hp2, hp3 and hp5 DNA mediated Au-Ag nanoparticles that were nanomushroom-like. Since two parts of Au and Ag were related but separated relatively, the

Table 1 DNA sequences used for conjugation with AuNPs

DNA strands	DNA sequence (5'→3')
hp1	SH-C6-TGG TCC GAT GTC TTT GAC ATC GGA CCA
hp2	SH-C6-TGG TCC GAT GTC TTT TTT TTG ACA TCGG ACC A
hp3	SH-C6-TGG TCC GAT GTC TTT TTT TTT TTT TTT GAC ATC GGA CCA
hp4	SH-C6-TGG TCC GAT TTT CGG ACC A
hp5	SH-C6-TGG TCC GAT GTC GAT CTT TGA TCG ACA TCG GAC CA

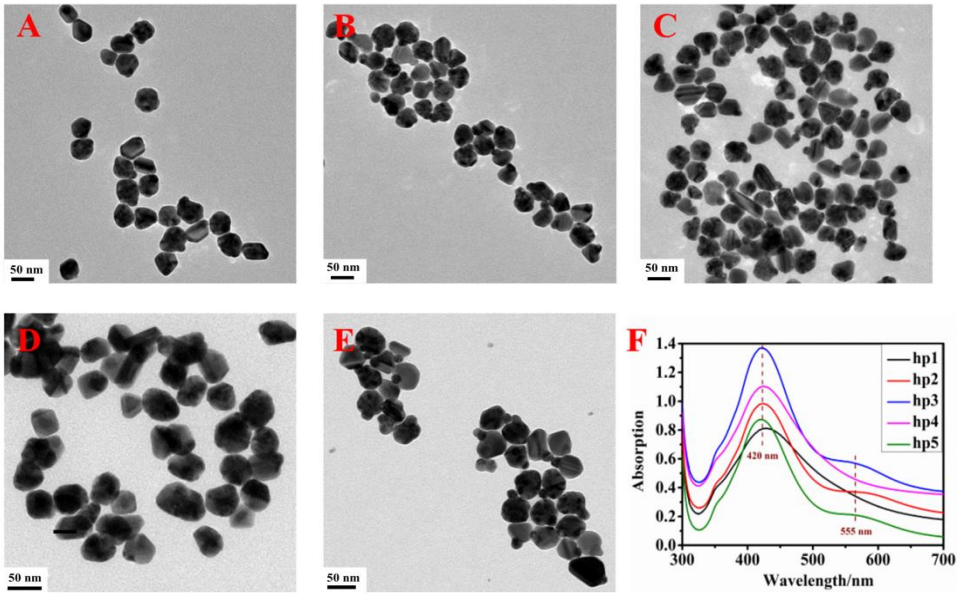

Fig. 3 TEM images of Au-Ag nanoparticles synthesized with different hp DNA, including hp1 (A), hp2 (B), hp3 (C), hp4 (D) and hp5 (E); UV-Vis spectra of Au-Ag nanoparticles mediated by these hp DNA (F)

plasma resonance of both Au and Ag were observed. Among them, 420 nm was attributed to the plasma resonance of Ag, and 555 nm was related to the plasma resonance of Au. In contrast, the UV-vis spectra of hp1 and hp4 DNA mediated Au-Ag nanoparticles that were not nanomushroom-like only had an resonance peak of 420 nm. Since the Au core was completely wrapped by the Ag shell in the Au-Ag core-shell structure, it was difficult to observe the plasma resonance of Au. Therefore, the resonance peak at ~555 nm was hard to be observed in the UV-Vis spectra of hp1 and hp4 DNA mediated Au-Ag core-shell nanoparticles. Moreover, by counting about 200 nanoparticles synthesized from three different batches, it was indicated that the yield of hp3 mediated Au-Ag nanomushrooms was more than 90% which was much higher than those of hp2 (~70%) and hp1 (~25%). The main reason was attributed to the bigger loop of hp3 sequence with 15 bases than 8-base and 3-base loop of hp2 and hp1 sequence, and to the longer stem of hp5 sequence with 16 bases than 12-base and 8-base stem of hp1 and hp4 sequence. The difference of hp DNA structure caused different steric stabilization and charge distribution on the surface of AuNPs, resulting in different morphologies of Au-Ag nanoparticles.

The loading amount of DNA on the AuNP surface is directly determined by the feed ratio, which is closely related to the surface charge distribution of AuNPs and steric hindrance between DNA sequences. Thus, various molar ratios of hp DNA were employed to synthesize hp DNA modified AuNPs. Different morphologies of hp DNA mediated Au-Ag nanoparticles with different molar ratios including 100:1, 200:1 and 400:1 were recorded by TEM and shown in Fig. 4. The number of DNA conjugated on AuNPs was calculated to 34, 47 and 101 respectively by Oligreen assay. It could be clearly seen that with the increasing loading amount of hp5 DNA on the surface of AuNPs, the number of resulted Au-Ag nanomushrooms increased significantly. Besides, nanoparticles were also characterized by UV-Vis Spectrometer and zeta electric potential analyzer, as shown in Figs. 4 and 5. It could be seen that with the increasing loading amount of hp5 DNA on the surface of AuNPs, the Zeta potential of hp5 DNA-AuNPs decreased from -1.88 mV to -14.34 mV, and the resulted Au-Ag nanoparticles were nanomushroom-like. In addition, when the loading amount of hp5 DNA increased from 34 to 101, the color of as-grown Au-Ag nanoparticles solution changed from yellow to pale green, as shown in the Fig. 6. And the UV-Vis spectrum of Au-Ag nanoparticles not only had the absorption peak of silver nanoparticle near 420 nm, but also had a new absorption peak near 555 nm. These results suggested that the morphology and plasmonic property of Au-Ag nanoparticles could be precisely tuned by changing the loading amount of hp DNA modified on AuNPs surface.

The stability of the Au-Ag nanomushrooms was evaluated by measuring their UV-Vis absorption spectrum during a 14-day testing period. It could be seen from Fig. 7 that their UV-Vis absorption spectrum remained basically consistent, indicating the excellent stability of the proposed Au-Ag nanomushrooms. In fact, it was observed that the Au-Ag nanomushrooms aqueous solution was well dispersed without aggregation for 1 month at least.

3.3 Formation mechanism of Au-Ag nanomushrooms

Based on these experimental results and previous research results, we proposed the following growth and formation mechanism of Au-Ag bimetallic nanomushrooms as Fig. 8. It is well known that DNA binding affinity and structural rigidity greatly affects the relative deposition and diffusion rate of metal atom, which ultimately determines the morphology of metal nanoparticles (Gilroy *et al*. 2016) (Satyavolu *et al*. 2016). Since hp DNA has better rigidity than single-stranded DNA and the affinity of base T to

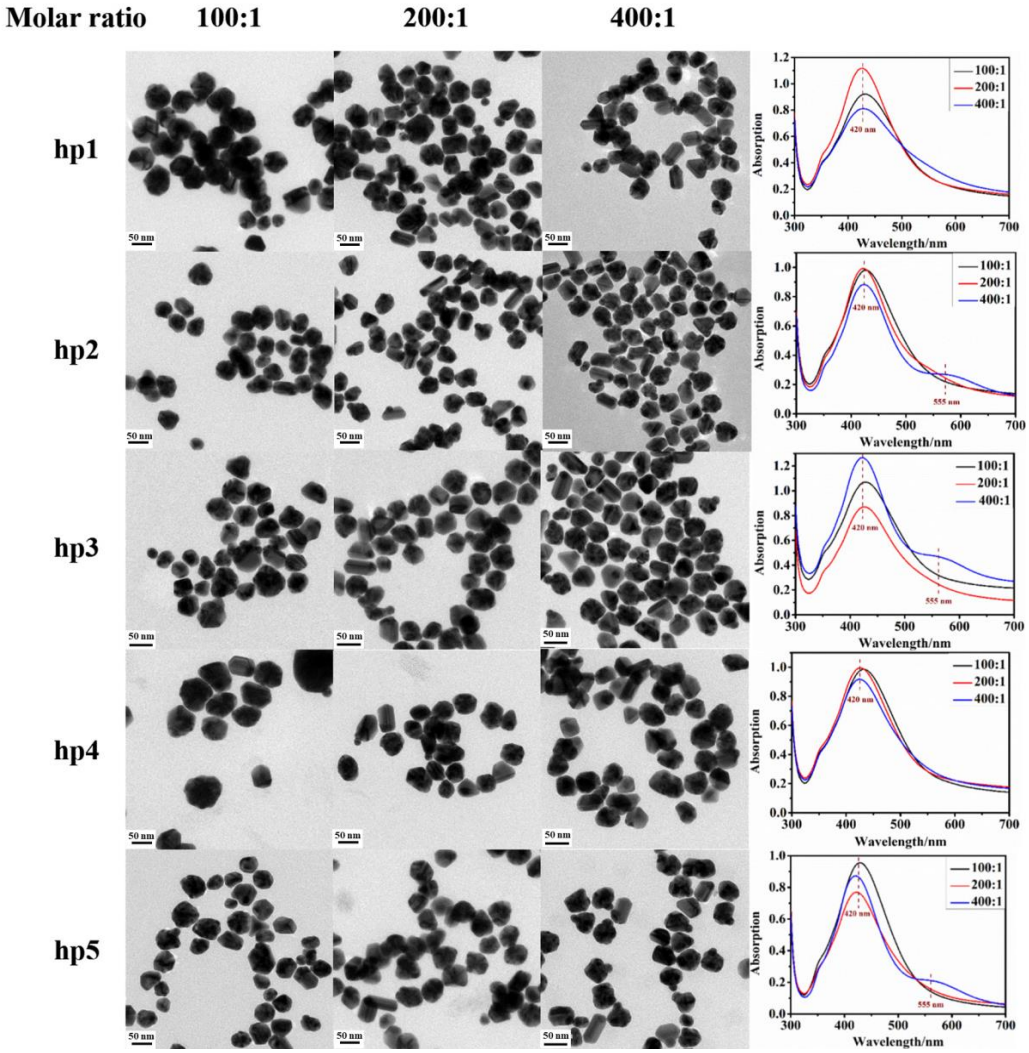

Fig. 4 TEM images and UV-vis spectra of hp DNA mediated Au-Ag nanoparticles with different molar ratios

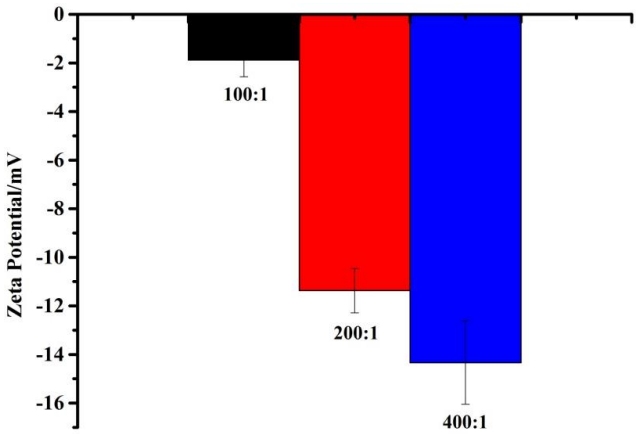

Fig. 5 The potential of hp5 DNA-AuNPs with different molar ratios

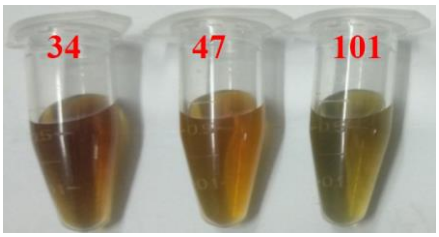

Fig. 6 Photographs of hp5 DNA-AuNPs with different loading amount

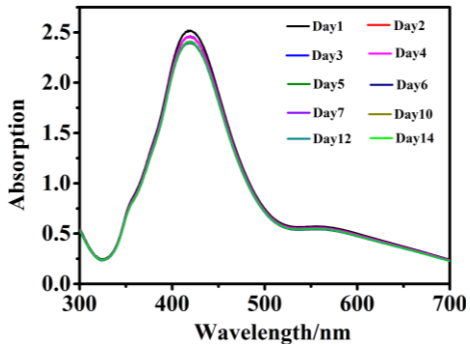

Fig. 7 UV-Vis absorption spectrum of Au-Ag nano-mushrooms aqueous solution during a 14-day testing period

AuNPs is weak, the template hp DNA would erect on the surface of AuNPs (Zhang *et al*. 2019) (Satyavolu *et al*. 2019). Besides, as shown in Fig. 8(A), the bigger loop of hp DNA on the surface of gold nanoseeds would lead to larger space between them, which would facilitate the introduction of large Ag-PVP complex (Zhang *et al*. 1996) and the

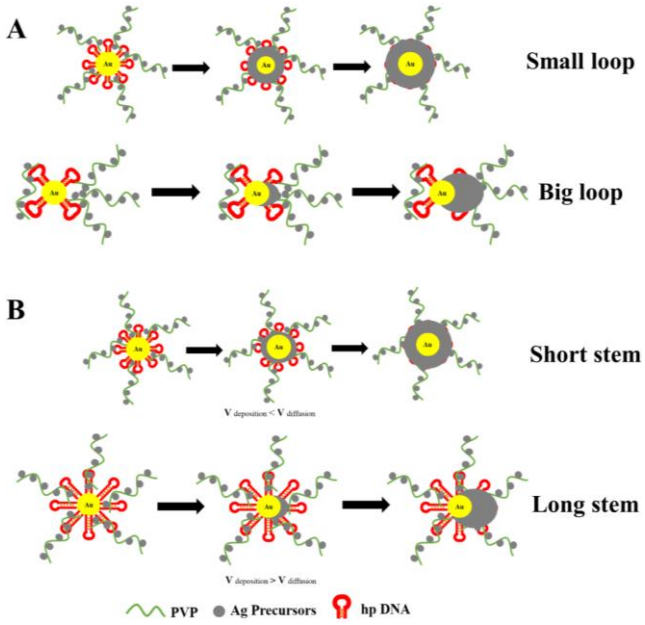

Fig. 8 Schematic diagram for the growth and formation mechanism of Au-Ag bimetallic nanomushrooms influenced by different hairpin DNA loop size (A) and stem length (B)

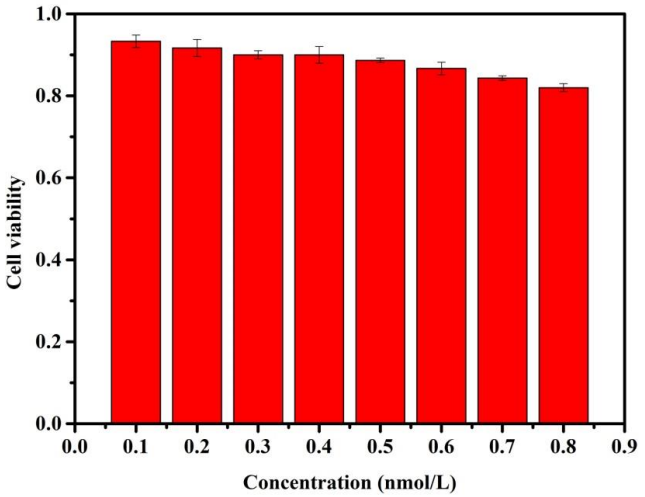

Fig. 9 Cell viability of HeLa cells incubated with various concentrations of Au-Ag nanomushrooms

deposition of Ag in a specific direction, resulting in the directional growth of Ag nanoparticles on gold nanoseeds. On the other hand, long-chain DNA induced the faster deposition rate of silver nanoparticles on gold nanoseeds than that of short-chain DNA (Lee *et al*. 2012). And hp DNA slowed down the diffusion rate of silver nanoparticles on the surface of gold nanoseeds, so hp DNA with long stem eventually generated the anisotropic mushroom-like structure, as shown in Fig. 8B. In contrast, when the loop of template hp DNA was small or the stem was short, hp DNA was evenly distributed on the surface of gold nanoseeds, forming multiple nucleation sites. Thus, the deposition rate of silver nanoparticles on the surface of gold nanoseeds was closed to their diffusion rate, resulting in the final core-shell structure. In addition, with the increase of DNA loading

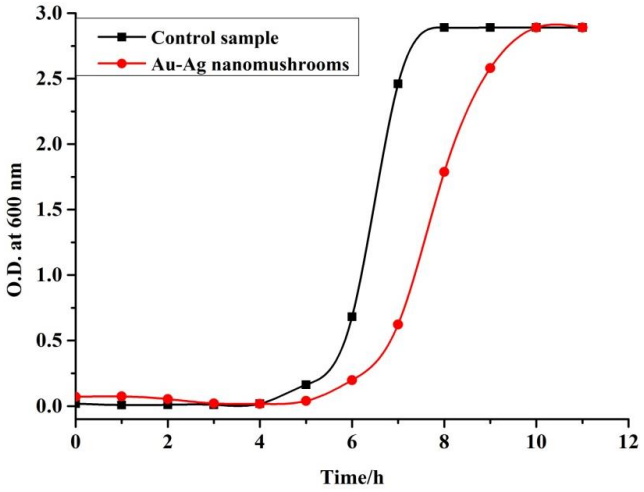

Fig. 10 The growth curve of E. coli by adding the antibacterial Au-Ag bimetallic nanomushrooms

amount, the DNA layer would block the deposition of silver nanoparticles on the surface of gold nanoseeds (Shen *et al*. 2015). When a nucleation site was formed, silver nanoparticles would deposit and grow at that point and finally led to the formation of Au-Ag bimetallic nanomushrooms, because silver was more likely to be deposited on the existing nucleation site (Gu *et al*. 2005).

3.4 Antibacterial Application of Au-Ag bimetallic nanomushrooms

Metal nanoparticles have been widely used as antibacterial agents (Li *et al*. 2016) or optical probes (Su *et al*. 2017) in biochemistry, due to their large specific surface area and good biocompatibility. Studies have shown that metal nanoparticles with different chemical compositions, morphologies and structures have different optical characteristics and antibacterial activities, which is due to the different surface plasmon resonance properties and the ability to generate reactive oxygen species (Guo *et al*. 2018) (Bhamidipati *et al*. 2017). The application of DNA mediated metal nanoparticles in biology and medicine has the advantages of low biotoxicity, easy labeling and modification.

In this study, the biocompatibility and antibacterial properties of Au-Ag bimetallic nanomushrooms using CCK-8 method and E. coli were investigated, respectively. The cell viability of HeLa cells incubated with various concentrations of Au-Ag nanomushrooms was shown in Fig. 9. The results showed that more than 82% cell viability was observed in the varying concentration ranges, which suggested that the proposed Au-Ag nanomushrooms possessed the excellent biocompatibility. The growth curve of E. coli was shown in Fig. 10. It could be seen that without the bacterial inhibitor, the rapid growth phase of E. coli emerged after 5 h of culture, and the stable phase appeared within 8 h. When the E. coli was cultured with Au-Ag bimetallic nanomushrooms for 6 h, the rapid growth phase and stable phase of E. coli appeared within 10 h. The results suggested that Au-Ag bimetallic nanomushrooms had good antibacterial properties and possessed the great potential as an antibacterical reagent in future.

4. Conclusions

In conclusion, a kind of Au-Ag bimetallic nanomushrooms was successfully synthesized by the hairpin DNA mediated method. Under the optimized synthesis conditions including the structure of template hairpin DNA, loading amounts of hairpin DNA, types of reductant agents and surfactants, Au-Ag bimetallic nanomushrooms exhibited specific morphology. Then, the formation mechanism of hairpin DNA mediated Au-Ag nanomushrooms was investigated and discussed. The biocompatibility of proposed Au-Ag bimetallic nanomushrooms was evaluated by a CCK-8 method, and Au-Ag bimetallic nanomushrooms exhibited low biotoxicity. Finally, the proposed Au-Ag bimetallic nanomushrooms with good biocompatibility were applied for the antibacterial study. These results suggested that the proposed Au-Ag bimetallic nanomushrooms possessed the potential to be excellent antibacterial agents for biomedical science in the future.

Acknowledgments

The research described in this paper was financially supported by the National Natural Science Foundation of China (Nos. 22074161 and 21976213), Guangdong Basic and Applied Basic Research Foundation (No.2019A1515010107), the Research and Development Plan for Key Areas of Food Safety in Guangdong Province of China (No. 2019B020211001), the Science and Technology Planning Project of Guangzhou City (No. 202102080167), and National Key Research and Development Program of China (No. 2019YFC1606101), respectively.

References

Berahim, N., Basirun, W.J., Leo, B.F. and Johan, M.R. (2018), "Synthesis of Bimetallic Gold-Silver (Au-Ag) Nanoparticles for the Catalytic Reduction of 4-Nitrophenol to 4-Aminophenol", *Catalysts*, **8**(10), 412. https://doi.org/10.3390/catal8100412.

Bhamidipati, M. and Fabris, L. (2017), "Multiparametric assessment of gold nanoparticle cytotoxicity in cancerous and healthy cells: The role of size, shape, and surface chemistry", *Bioconjugate Chem.*, **28**(2), 449-460. https://doi.org/10.1021/acs.bioconjchem.6b00605.

Chen, Z., Liu, C., Cao, F., Ren, J. and Qu, X. (2018), "DNA metallization: principles, methods, structures, and applications", *Chem. Soc. Rev.*, **47**(11), 4017-4072. https://xs.scihub.ltd/10.1039/C8CS00011E.

Chi, M., Wang, C., Lei, Y., Wang, G., Li, D., More, K.L., Lupini, A., Allard, L.F., Markovic, N.M. and Stamenkovic, V.R. (2015), "Surface faceting and elemental diffusion behaviour at atomic scale for alloy nanoparticles during in situ annealing", *Nature Commun.*, **6**, 8925. https://xs.scihub.ltd/https://doi.org/10.1038/ncomms9925.

Da Silva, A.G.M., Rodrigues, T.S., Haigh, S.J. and Camargo, P.H.C. (2017), "Galvanic replacement reaction: recent developments for engineering metal nanostructures towards catalytic applications", *Chem. Commun.*, **53**(53), 7135-7148. https://xs.scihub.ltd/10.1039/C7CC02352A.

Demers, L.M., Mirkin, C.A., Mucic, R.C., Reynolds, R.A., Letsinger, R.L., Elghanian, R. and Viswanadham, G. (2000), "A fluorescence-based method for determining the surface coverage and hybridization efficiency of thiol-capped oligonucleotides bound to gold thin films and nanoparticles", *Anal. Chem.*, **72**(22), 5535-5541. https://pubs.acs.org/doi/10.1021/ac0006627.

Fan, Z. and Zhang, H. (2016), "Template synthesis of noble metal nanocrystals with unusual crystal structures and their catalytic applications. Accounts of chemical research", *Accounts Chem. Res.*, **49**(12), 2841-2850. https://doi.org/10.1021/acs.accounts.6b00527.

Fu, J., Zhang, Z. and Li, G. (2019), "Progress on the development of DNA-mediated metal nanomaterials for environmental and biological analysis", *Chinese Chem. Lett.*, **30**(2), 285-291. https://doi.org/10.1016/j.cclet.2018.10.031.

Gilroy, K.D., Ruditskiy, A., Peng, H., Qin, D. and Xia, Y. (2016), "Bimetallic nanocrystals: Syntheses, properties, and applications", *Chem. Rev.*, **116**(18), 10414-10472. https://doi.org/10.1021/acs.chemrev.6b00211.

Gu, H.W., Yang, Z.M., Gao, J.H., Chang, C.K., and Xu, B. (2005), "Heterodimers of nanoparticles: Formation at a liquid-liquid interface and particle-specific surface modification by functional molecules", *J. Am. Chem. Soc.*, **127**(1), 34-35. https://doi.org/10.1021/ja045220h.

Guo, R., Yin, F., Sun, Y., Mi, L., Shi, L., Tian, Z. and Li, T. (2018), "Ultrasensitive simultaneous detection of multiplex disease-related nucleic acids using double-enhanced surface-enhanced Raman scattering nanosensors", *ACS Appl. Mater. Interfac.*, **10**(30), 25770-25778. https://doi.org/10.1021/acsami.8b06757.

Habibi, M.H., Kamrani, R. and Mokhtari, R. (2010), "Fabrication and characterization of copper nanoparticles using thermal reduction: The effect of nonionic surfactants on size and yield of nanoparticles", *Microchim. Acta*. **171**(1-2), 91-95. https://doi.org/10.1007/s00604-010-0413-2.

Han, L., Li, C., Zhang, T., Lang, Q. and Liu, A. (2015), "Au@ Ag heterogeneous nanorods as nanozyme interfaces with peroxidase-like activity and their application for one-pot analysis of glucose at nearly neutral pH", *ACS Appl. Mater. Interfac.*, **7**(26), 14463-14470. https://doi.org/10.1021/acsami.5b03591.

Jawad, M., Ali, S., Waseem, A., Rabbani, F., Amin, B.A.Z., Bilal, M. and Shaikh, A.J. (2019), "Plasmonic effects and size relation of gold-platinum alloy nanoparticles", *Adv. Nano Res.*, **7**(3)**,** 167-178. https://doi.org/10.12989/anr.2019.7.3.167.

Kim, S.J., Choi, S.J., Jang, J.S., Cho, H.J., Koo, W.T., Tuller, H.L. and Kim, I.D. (2017), "Exceptional high-performance of Pt-based bimetallic catalysts for exclusive detection of exhaled biomarkers", *Adv. Mater.*, **29**(36), 1700737. https://doi.org/10.1002/adma.201700737.

Lee, J.H., Kim, G.H. and Nam, J.M. (2012), "Directional synthesis and assembly of bimetallic nanosnowmen with DNA", *J. Am. Chem. Soc.*, **134**(12), 5456-5459. https://doi.org/10.1021/ja2121525.

Lee, J.H., You, M.H., Kim, G.H. and Nam, J.M. (2014), "Plasmonic nanosnowmen with a conductive junction as highly tunable nanoantenna structures and sensitive, quantitative and multiplexable surface-enhanced Raman scattering probes", *Nano Lett.*, **14**(11), 6217-6225. https://doi.org/10.1021/nl502541u.

Li, J., Zhu, Z., Liu, F., Zhu, B., Ma, Y., Yan, J., Lin, B., Ke, G., Liu, R., Zhou, L., Tu. S. and Yang. C. (2016), "DNA-mediated morphological control of silver nanoparticles", *Small*, **12**(39), 5449-5487. https://doi.org/10.1002/smll.201601338.

Li, S., Wei, T., Tang, M., Chai, F., Qu, F. and Wang, C. (2018), "Facile synthesis of bimetallic Ag-Cu nanoparticles for colorimetric detection of mercury ion and catalysis", *Sensor*

Actuat. B Chem., **255,** 1471-1481. https://doi.org/10.1016/j.snb.2017.08.159.

Lim, D., Kim, I. and Nam, J. (2008), "DNA-embedded Au/Ag core-shell nanoparticles", *Chem. Commun.* (42), 5312-5314. https://xs.scihub.ltd/10.1039/B810195G.

Liz Marzan, L.M. (2006), "Tailoring surface plasmons through the morphology and assembly of metal nanoparticles", *Langmuir*, **22**(1), 32-41. https://doi.org/10.1021/la0513353.

Lu, X., Tao, L., Song, D., Li, Y. and Gao, F. (2018), "Bimetallic Pd@Au nanorods based ultrasensitive acetylcholinesterase biosensor for determination of organophosphate pesticides", *Sensor Actuat. B Chem.*, **255,** 2575-2581. https://doi.org/10.1016/j.snb.2017.09.063.

Ma, X., Huh, J., Park, W., Lee, L.P., Kwon, Y. J. and Sim, S.J. (2016), "Gold nanocrystals with DNA-directed morphologies", *Nature Commun.*, **7**(1), 1-8. https://doi.org/10.1038/ncomms12873.

Ma, Y., Wu, X. and Zhang, G. (2017), "Core-shell Ag@Pt nanoparticles supported on sepiolite nanofibers for the catalytic reduction of nitrophenols in water: Enhanced catalytic performance and DFT study", *Appl. Catal. B Environ.*, **205**, 262-270. https://doi.org/10.1016/j.apcatb.2016.12.025.

Madsen, M. and Gothelf, K.V. (2019), "Chemistries for DNA nanotechnology", *Chem. Rev.*, **119**(10), 6384-6458. https://doi.org/10.1021/acs.chemrev.8b00570.

Mandal, R., Baranwal, A., Srivastava, A. and Chandra, P. (2018), "Evolving trends in bio/chemical sensor fabrication incorporating bimetallic nanoparticles", *Biosens. Bioelectron.*, **117**, 546-561. https://doi.org/10.1016/j.bios.2018.06.039.

Martinsson, E., Shahjamali, M.M., Large, N., Zaraee, N., Zhou, Y., Schatz, G.C., Mirkin, C.A. and Aili, D. (2016), "Influence of surfactant bilayers on the refractive index sensitivity and catalytic properties of anisotropic gold nanoparticles", *Small*, **12**(3), 330-342. https://doi.org/10.1002/smll.201502449.

Niu, Z., Cui, F., Yu, Y., Becknell, N., Sun, Y., Khanarian, G., Kim, D., Dou, L., Dehestani, A., Schierle Arndt, K. and Yang. P. (2017), "Ultrathin epitaxial Cu@ Au core–shell nanowires for stable transparent conductors", *J. Am. Chem. Soc.*, **139**(21), 7348-7354. https://doi.org/10.1021/jacs.7b02884.

Satyavolu, N.S.R., Tan, L.H. and Lu, Y. (2016), "DNA-mediated morphological control of Pd–Au bimetallic nanoparticles", *J. Am. Chem. Soc.*, **138**(50), 16542-16548. https://doi.org/10.1021/jacs.6b10983.

Satyavolu, N.S.R., Loh, K.Y., Tan, L.H. and Lu, Y. (2019), "Discovery of and insights into DNA "codes" for tunable morphologies of metal nanoparticles", *Small*, **15**(26), 1900975. https://doi.org/10.1002/smll.201900975.

Shen, J., Su, J., Yan, J., Zhao, B., Wang, D., Wang, S., Li, K., Liu, M., He, Y., Mathur, S., Fan, C. and Song, S. (2015), "Bimetallic nano-mushrooms with DNA-mediated interior nanogaps for high-efficiency SERS signal amplification", *Nano Res.*, **8**(3), 731-742. https://doi.org/10.1007/s12274-014-0556-2.

Song, T., Tang, L., Tan, L. H., Wang, X., Satyavolu, N. S. R., Xing, H., Wang, Z., Li, J., Liang, H. and Lu, Y. (2015), "DNA-encoded tuning of geometric and plasmonic properties of nanoparticles growing from gold nanorod seeds", *Angew. Chem. Int. Edit.*, **54**(28), 8114-8118. https://doi.org/10.1002/anie.201500838.

Su, J., Wang, D., Nörbel, L., Shen, J., Zhao, Z., Dou, Y., Peng, T., Shi, J., Mathur, S., Fan C. and Song, S. (2017), "Multicolor gold–silver nano-mushrooms as ready-to-use SERS probes for ultrasensitive and multiplex DNA/miRNA detection", *Anal. Chem.*, **89**(4), 2531-2538. https://doi.org/10.1021/acs.analchem.6b04729.

Tan, L.H., Yue, Y., Satyavolu, N.S.R., Ali, A.S., Wang, Z., Wu, Y. and Lu, Y. (2015), "Mechanistic insight into DNA-guided control of nanoparticle morphologies", *J. Am. Chem. Soc.*, **137**(45), 14456-14464. https://doi.org/10.1021/jacs.5b09567.

Taylor, A.K., Perez, D.S., Zhang, X., Pilapil, B.K., Engelhard, M.H., Gates, B.D. and Rider, D.A. (2017), "Block copolymer templated synthesis of Ptlr bimetallic nanocatalysts for the formic acid oxidation reaction", *J. Mater. Chem. A*, **5**(40)**,** 21514-21527. https://xs.scihub.ltd/10.1039/C7TA06458F.

Wang, H., Qiao, X., Chen, J., Wang, X. and Ding, S. (2005), "Mechanisms of PVP in the preparation of silver nanoparticles", *Mater. Chem. Phys.*, **94**(2-3), 449-453. https://doi.org/10.1016/j.matchemphys.2005.05.005.

Wang, Z., Zhang, J., Ekman, J. M., Kenis, P.J. and Lu, Y. (2010), "DNA-mediated control of metal nanoparticle shape: one-pot synthesis and cellular uptake of highly stable and functional gold nanoflowers", *Nano Lett.*, **10**(5), 1886-1891. https://doi.org/10.1021/nl100675p.

Wang, P., Lin, Z., Su, X. and Tang, Z. (2017), "Application of Au based nanomaterials in analytical science", *Nano Today*, **12**, 64-97. https://doi.org/10.1016/j.nantod.2016.12.009.

Xia, Y., Gilroy, K.D., Peng, H.C. and Xia, X. (2017), "Seed-mediated growth of colloidal metal nanocrystals", *Angew. Chem. Int. Edit.*, **56**(1), 60-95. https://doi.org/10.1002/anie.201604731.

Yatsunyk, L.A., Mendoza, O. and Mergny, J. (2014), ""Nano-oddities": unusual nucleic acid assemblies for DNA-based nanostructures and nanodevices", *Accounts Chem. Res.*, **47**(6), 1836-1844. https://doi.org/10.1021/ar500063x.

Yin, Z., Wang, Y., Song, C., Zheng, L., Ma, N., Liu, X., Li, S., Lin, L., Li, M., Xu, Y., Li, W., Hu, G., Fang, Z. and Ma, D. (2018), "Hybrid Au–Ag nanostructures for enhanced plasmon-driven catalytic selective hydrogenation through visible light irradiation and surface-enhanced Raman scattering", *J. Am. Chem. Soc.*, **140**(3)**,** 864-867. https://doi.org/10.1021/jacs.7b11293.

Zaleska Medynska, A., Marchelek, M., Diak, M. and Grabowska, E. (2016), "Noble metal-based bimetallic nanoparticles: the effect of the structure on the optical, catalytic and photocatalytic properties", *Adv. Colloid. Interfac.*, **229,** 80-107. https://doi.org/10.1016/j.cis.2015.12.008.

Zhang, Z., Zhao, B. and Hu, L. (1996), "PVP protective mechanism of ultrafine silver powder synthesized by chemical reduction processes", *J. Solid St. Chem.*, **121**(1), 105-110. https://doi.org/10.1006/jssc.1996.0015.

Zhang, Y., Yang, P., Habeeb Muhammed, M.A., Alsaiari, S.K., Moosa, B., Almalik, A., Kumar, A., Ringe, E. and Khashab, N.M. (2017), "Tunable and linker free nanogaps in core–shell plasmonic nanorods for selective and quantitative detection of circulating tumor cells by SERS. ACS applied materials & interfaces", *ACS Appl. Mater. Interfac.*, **9**(43), 37597-37605. https://doi.org/10.1021/acsami.7b10959.

Zhang, Y., Wang, G., Yang, L., Wang, F. and Liu, A. (2018), "Recent advances in gold nanostructures based biosensing and bioimaging", *Coordination Chem. Rev.*, **370**, 1-21. https://doi.org/10.1016/j.ccr.2018.05.005.

Zhang, Z., Gao, J., Yu, Z. and Li, G. (2019), "Synthesis of tunable DNA-directed trepang-like Au nanocrystals for imaging application", *Nanoscale*, **11**(39), 18099-18108. https://xs.scihub.ltd/10.1039/C9NR06375G.

Zhao, J., Long, L., Weng, G., Li, J., Zhu, J. and Zhao, J. (2017), "Multi-branch Au/Ag bimetallic core-shell-satellite nanoparticles as a versatile SERS substrate: The effect of Au branches in a mesoporous silica interlayer", *J. Mater. Chem. C*, **5**(48), 12678-12687. https://xs.scihub.ltd/10.1039/C7TC03788K.

JL